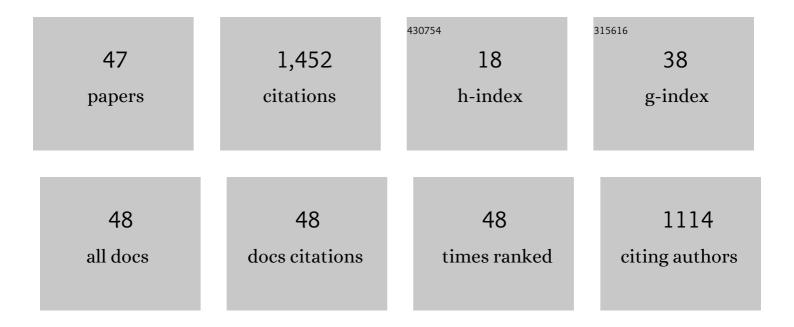
Yutaro Takaya

List of Publications by Year in descending order

Source: https://exaly.com/author-pdf/9118683/publications.pdf Version: 2024-02-01



#	Article	IF	CITATIONS
1	Re–Os geochemistry of hydrothermally altered dacitic rock in a submarine volcano at Site U1527, IODP Expedition 376: Implications for the Re cycle in intraoceanic arcs. Deep-Sea Research Part I: Oceanographic Research Papers, 2022, 180, 103687.	0.6	2
2	Umber as a lithified REY-rich mud in Japanese accretionary complexes and its implications for the osmium isotopic composition of Middle Cretaceous seawater. Ore Geology Reviews, 2022, 142, 104683.	1.1	5
3	Derivation of Flotation Kinetic Model Combining Surface Property Analysis and Kinetics. Journal of MMIJ, 2022, 138, 12-18.	0.4	0
4	Prediction of Acid Mine Drainage Treatment by Open Limestone-Alkaline Material Channel and Implications for the Large Scale Implementation of Passive Treatment. Journal of MMIJ, 2022, 138, 19-27.	0.4	3
5	Mechanochemical degradation treatment of TBBPA: A kinetic approach for predicting the degradation rate constant. Advanced Powder Technology, 2022, 33, 103469.	2.0	4
6	Impact of Biodegradable Plastics, Especially PHBH, on Mechanical Recycling. Resources Processing, 2022, 68, 143-149.	0.4	1
7	Formation of highly Zn-enriched sulfide scale at a deep-sea artificial hydrothermal vent, Iheya-North Knoll, Okinawa Trough. Mineralium Deposita, 2021, 56, 975.	1.7	6
8	A Combination of Geostatistical Methods and Principal Components Analysis for Detection of Mineralized Zones in Seafloor Hydrothermal Systems. Natural Resources Research, 2021, 30, 2875-2887.	2.2	11
9	Purification of calcium fluoride (CaF2) sludge by selective carbonation of gypsum. Journal of Environmental Chemical Engineering, 2021, 9, 104510.	3.3	6
10	Marine osmium isotope record during the Carnian "pluvial episode―(Late Triassic) in the pelagic Panthalassa Ocean. Global and Planetary Change, 2021, 197, 103387.	1.6	33
11	Subseafloor sulphide deposit formed by pumice replacement mineralisation. Scientific Reports, 2021, 11, 8809.	1.6	17
12	Progressive ocean oxygenation atÂ~2.2ÂGa inferred from geochemistry and molybdenum isotopes of the Nsuta Mn deposit, Ghana. Chemical Geology, 2021, 567, 120116.	1.4	6
13	3D geostatistical modeling of metal contents and lithofacies for mineralization mechanism determination of a seafloor hydrothermal deposit in the middle Okinawa Trough, Izena Hole. Ore Geology Reviews, 2021, 135, 104194.	1.1	6
14	Removal mechanisms of arsenite by coprecipitation with ferrihydrite. Journal of Environmental Chemical Engineering, 2021, 9, 105819.	3.3	21
15	Kinetic Evaluation of pH and Temperature Effects on Silica Polymerization in the Presence of Mg, Al and Fe. Kagaku Kogaku Ronbunshu, 2021, 47, 237-244.	0.1	1
16	Fish proliferation and rare-earth deposition by topographically induced upwelling at the late Eocene cooling event. Scientific Reports, 2020, 10, 9896.	1.6	29
17	Quantitative in situ mapping of elements in deep-sea hydrothermal vents using laser-induced breakdown spectroscopy and multivariate analysis. Deep-Sea Research Part I: Oceanographic Research Papers, 2020, 158, 103232.	0.6	28
18	Biotic and environmental changes in the Panthalassa Ocean across the Norian (Late Triassic) impact event. Progress in Earth and Planetary Science, 2020, 7, .	1.1	8

ΥUTARO ΤΑΚΑΥΑ

#	Article	IF	CITATIONS
19	Unique Environmental Conditions Required for Dawsonite Formation: Implications from Dawsonite Synthesis Experiments under Alkaline Conditions. ACS Earth and Space Chemistry, 2019, 3, 285-294.	1.2	3
20	Experiments on Rare-Earth Element Extractions from Umber Ores for Optimizing the Grinding Process. Minerals (Basel, Switzerland), 2019, 9, 239.	0.8	3
21	Triassic marine Os isotope record from a pelagic chert succession, Sakahogi section, Mino Belt, southwest Japan. Journal of Asian Earth Sciences: X, 2019, 1, 100004.	0.6	7
22	A Miocene impact ejecta layer in the pelagic Pacific Ocean. Scientific Reports, 2019, 9, 16111.	1.6	15
23	Signal preprocessing of deep-sea laser-induced plasma spectra for identification of pelletized hydrothermal deposits using Artificial Neural Networks. Spectrochimica Acta, Part B: Atomic Spectroscopy, 2018, 145, 1-7.	1.5	26
24	The tremendous potential of deep-sea mud as a source of rare-earth elements. Scientific Reports, 2018, 8, 5763.	1.6	157
25	Longâ€Term Reaction Characteristics of CO ₂ –Water–Rock Interaction: Insight into the Potential Groundwater Contamination Risk from Underground CO ₂ Storage. Resource Geology, 2018, 68, 93-100.	0.3	5
26	A new and prospective resource for scandium: Evidence from the geochemistry of deep-sea sediment in the western North Pacific Ocean. Ore Geology Reviews, 2018, 102, 260-267.	1.1	41
27	Origin of felsic volcanism in the Izu arc intra-arc rift. Contributions To Mineralogy and Petrology, 2017, 172, 1.	1.2	13
28	Depositional Age of a Fossil Whale Bone from São Paulo Ridge, South Atlantic Ocean, Based on Os Isotope Stratigraphy of a Ferromanganese Crust. Resource Geology, 2017, 67, 442-450.	0.3	6
29	Rapid growth of mineral deposits at artificial seafloor hydrothermal vents. Scientific Reports, 2016, 6, 22163.	1.6	44
30	Major and trace element compositions and resource potential of ferromanganese crust at Takuyo Daigo Seamount, northwestern Pacific Ocean. Geochemical Journal, 2016, 50, 527-537.	0.5	26
31	Discovery of extremely REY-rich mud in the western North Pacific Ocean. Geochemical Journal, 2016, 50, 557-573.	0.5	68
32	Geochemistry of REY-rich mud in the Japanese Exclusive Economic Zone around Minamitorishima Island. Geochemical Journal, 2016, 50, 575-590.	0.5	42
33	Geological factors responsible for REY-rich mud in the western North Pacific Ocean: Implications from mineralogy and grain size distributions. Geochemical Journal, 2016, 50, 591-603.	0.5	46
34	Post-Drilling Changes in Seabed Landscape and Megabenthos in a Deep-Sea Hydrothermal System, the Iheya North Field, Okinawa Trough. PLoS ONE, 2015, 10, e0123095.	1.1	41
35	REY-Rich Mud. Fundamental Theories of Physics, 2015, , 79-127.	0.1	17
36	Dissolution of altered tuffaceous rocks under conditions relevant for CO2 storage. Applied Geochemistry, 2015, 58, 78-87.	1.4	8

ΥUTARO ΤΑΚΑΥΑ

#	Article	IF	CITATIONS
37	Re–Os isotope geochemistry in the surface layers of ferromanganese crusts from the Takuyo Daigo Seamount, northwestern Pacific Ocean. Geochemical Journal, 2015, 49, 233-241.	0.5	23
38	Rare-earth, major, and trace element geochemistry of deep-sea sediments in the Indian Ocean: Implications for the potential distribution of REY-rich mud in the Indian Ocean. Geochemical Journal, 2015, 49, 621-635.	0.5	51
39	Chemical leaching of rare earth elements from highly REY-rich mud. Geochemical Journal, 2015, 49, 637-652.	0.5	15
40	Uranium isotope systematics of ferromanganese crusts in the Pacific Ocean: Implications for the marine 238U/235U isotope system. Geochimica Et Cosmochimica Acta, 2014, 146, 43-58.	1.6	85
41	Zircon U–Pb dating from the mafic enclaves in the Tanzawa Tonalitic Pluton, Japan: Implications for arc history and formation age of the lower-crust. Lithos, 2014, 196-197, 301-320.	0.6	14
42	A Study on the Recovery Method of Rare-Earth Elements from REY-Rich Mud toward the Development and the Utilization of REY-Rich Mud. Journal of MMIJ, 2014, 130, 104-114.	0.4	15
43	Postâ€drilling changes in fluid discharge pattern, mineral deposition, and fluid chemistry in the Iheya North hydrothermal field, Okinawa Trough. Geochemistry, Geophysics, Geosystems, 2013, 14, 4774-4790.	1.0	52
44	Geological, geochemical and social-scientific assessment of basaltic aquifers as potential storage sites for CO2. Geochemical Journal, 2013, 47, 385-396.	0.5	7
45	Simplified Prediction of the Proceeding of Mineral Trapping of CO2 Based on Experimental Study. Journal of MMIJ, 2012, 128, 94-102.	0.4	Ο
46	Deep-sea mud in the Pacific Ocean as a potential resource for rare-earth elements. Nature Geoscience, 2011, 4, 535-539.	5.4	434
47	Geochemical Trapping of CO2 in Basaltic Aquifers: Implications from CO2-Water-Rock Interaction Experiments. Journal of MMIJ, 2010, 126, 131-137.	0.4	1